Spiral Galaxies

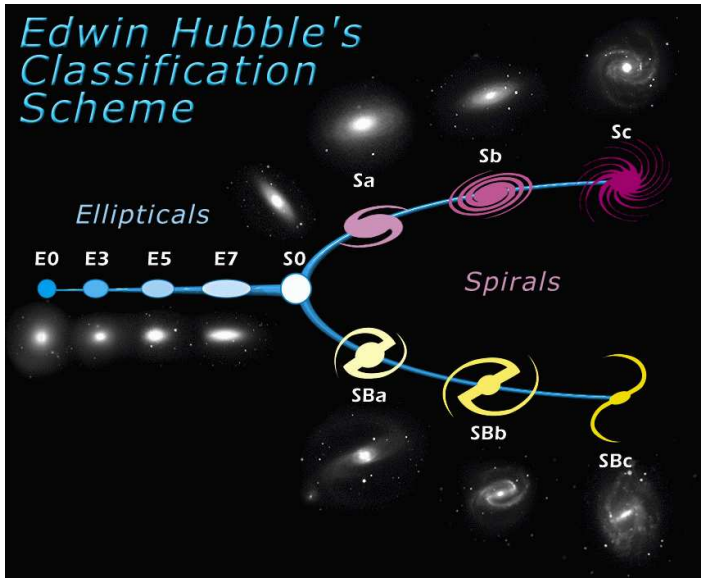

SDSS

Galaxy classification via the Hubble “tuning fork diagram”: “early types”: elliptical galaxies; “late types”: spiral galaxies.

Spiral Galaxies

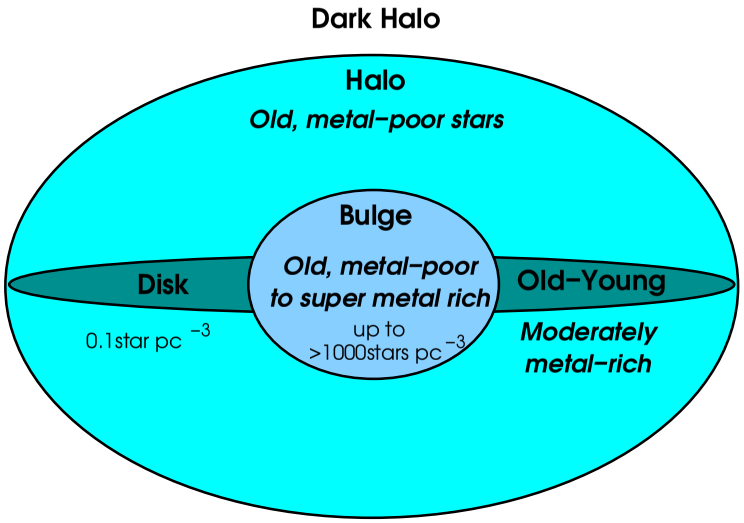

(after Prantzos, 2008; Pagel, 2009)

Spiral Galaxies

Despite many problems, it is often possible to roughly classify stars into different populations:

Population	Typical stars	Velocity Disp. (km s^{-1})	Shape	Abundance wrt. H
Halo pop. II	globular clusters red giants	130	spherical	0.003
Intermediate pop. II	high-v stars	50	intermediate	0.01
Disk pop.		30	intermediate	0.02
Intermediate pop. I	stars with strong lines	20	intermediate	0.03
Extreme pop. I	blue supergiants	10	Flat	0.04

after Combes et al.

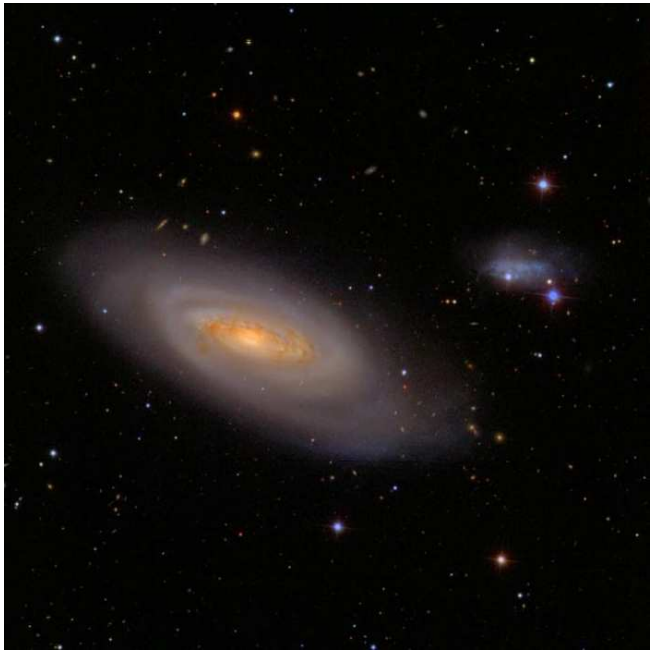

Optical light: emission from Galaxies is dominated by emission from

- stars
- emission nebulae

M90 (SDSS)

Starlight

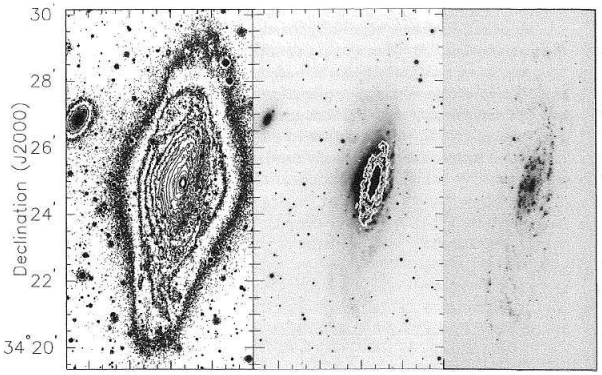

Left: R-band isophotes of NGC 7331, Middle: R-band image & CO emission, Right: Hα (SG Fig. 5.3).

There is lots of structure on galaxy images:
Bulge: circular isophotes $\Longrightarrow$ spherical distribution
Disk: isophotes elliptical $\Longrightarrow$ projection effect
inclination: $\sim 75^\circ$

Disk

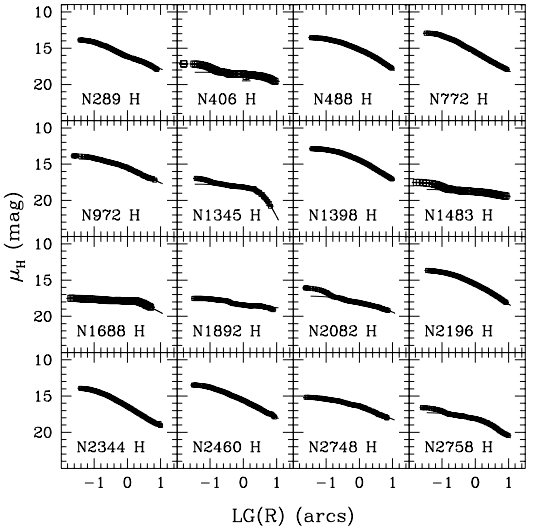

To get rid of structure: average over disk $\Longrightarrow$ surface brightness profile

(Seigar et al., 2002, Fig. 1a)

Disk

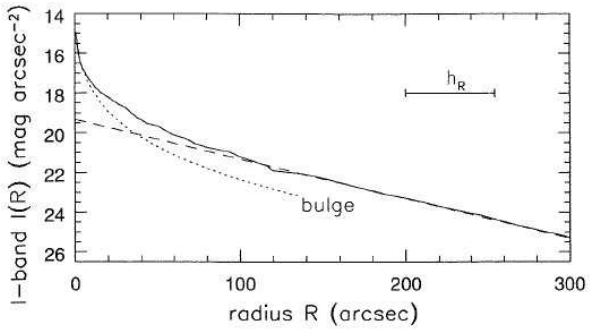

NGC7331: Surface brightness in I-band ($\sim$8000Å) (SG, Fig. 5.4);
Note: magnitudes are logarithmic: 5 mag = factor 100!

Generally surface brighness given in mag arcsec^{-2}, which is independent of distance.

For historical reasons edge of disk defined as where $I_B = 25$ mag arcsec^{-2} (R_{25}-radius)

Also sometimes used: Holmberg-radius ($I_B = 26.5$ mag arcsec^{-2})

For many spirals disk component well modeled by

$$I(R) = I_0 \exp(-R/h_R) \qquad (4.1)$$

where scale length 1 kpc $\lesssim h_R \lesssim$ 10 kpc and where typically $I_{0,B} \sim 22$ mag arcsec^{-2}.

Note that surface brightness is higher by $1/\cos i$ when disk is tilted.

R. Gendler

Bulge: well described by de Vaucouleurs' law:

$$\log\left(\frac{I(R)}{I_e}\right) = -3.3307\left[\left(\frac{R}{R_e}\right)^{1/4} - 1\right] \qquad (4.3)$$

where R_e: effective radius, i.e., radius containing in half of the total luminosity

This law is also valid for ellipticals

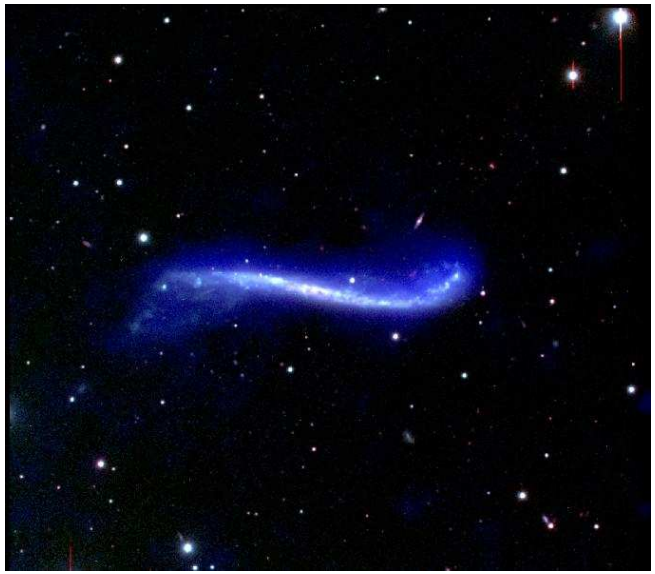

UGC 3697 ("Integral sign galaxy", a superthin galaxy; NRAO/AUI)

Vertical structure (z-direction): surface brightness well described by

$$I(R,z) = I(R)\exp\left\{-\frac{|z|}{h_z}\right\} \quad \text{where} \quad h_z \sim 0.1 h_R \qquad (4.2)$$

Sequence of Disk Galaxies

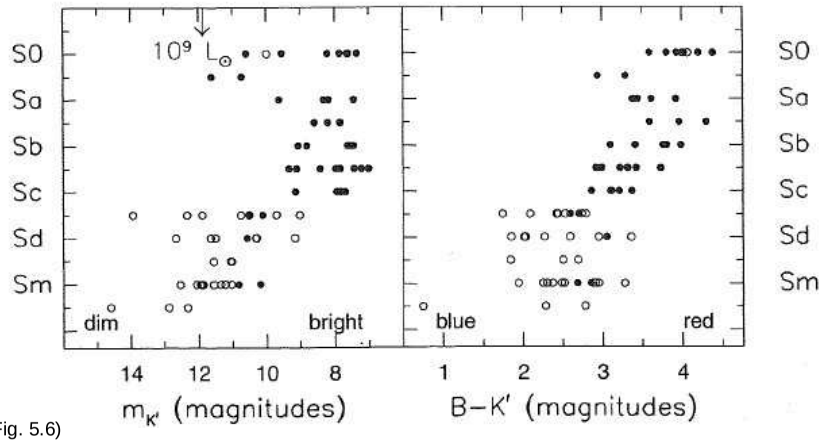

SG (Fig. 5.6)

S0 galaxies are luminous and red, while Sc and later are fainter and bluer

Sd: no bulge visible, Sm: Magellanic systems

Sequence of Disk Galaxies

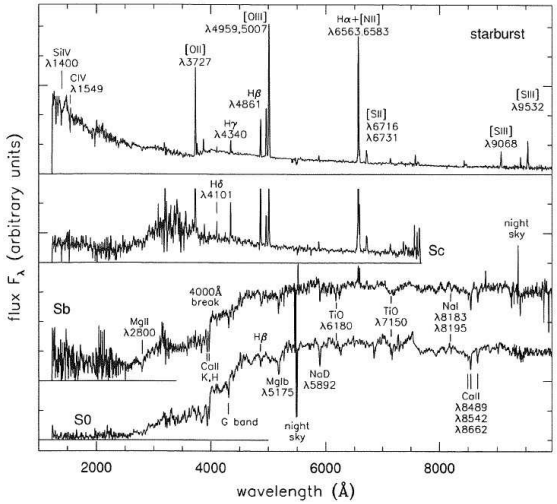

SG (Fig. 5.24)

galaxy spectra = $\sum$ constituent spectra

- S0: mainly absorption lines from cool K stars, Ca H, K from G-type stars
- Sc: mainly blue and UV emission, i.e., hot and young stars; emission lines from photoionized emission nebulae
- Starburst: significant photoionization present (see later)

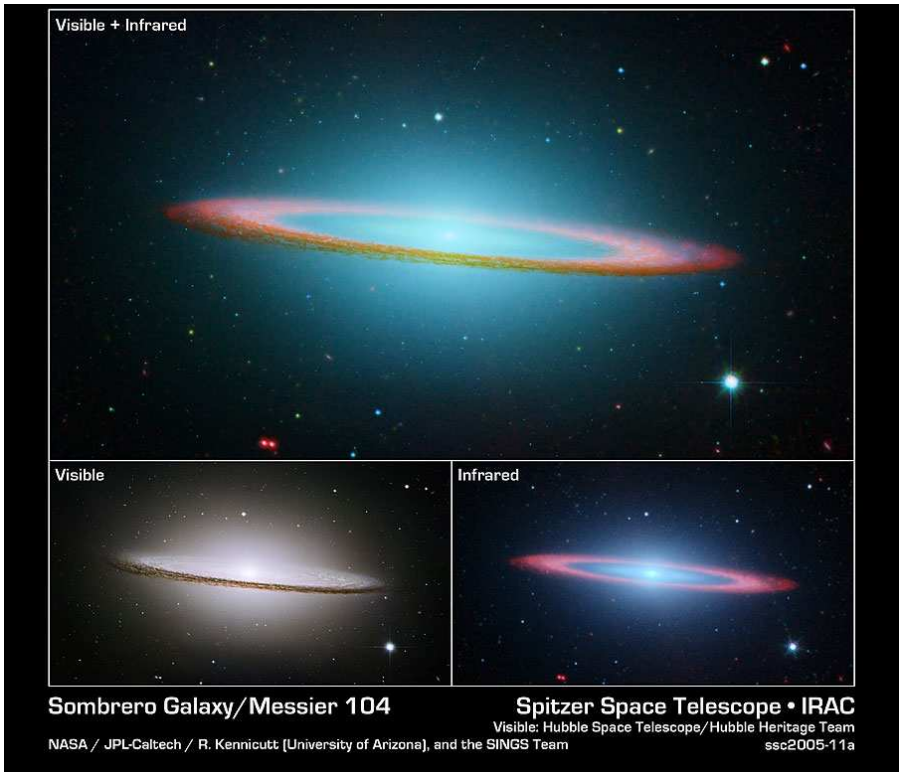

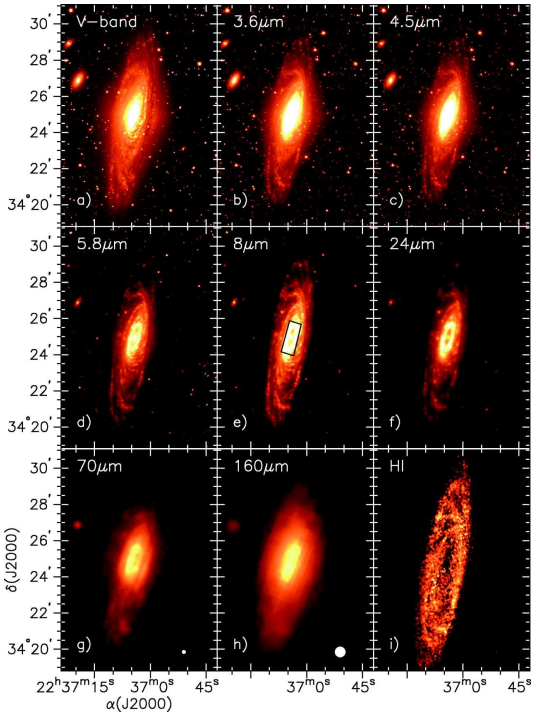

Multi-Color Image of NGC 7331, ISM mass is $5 \times 10^9\, M_\odot$.

Distribution of gas in disk mainly done using 21 cm imaging, dust using IR observations

We can generally trace H I to 10^{19} H atoms cm^{-2}, or $\sim$0.1 $M_\odot$ pc^{-2}.

(Regan et al., 2004)

Distribution of Gas and Dust

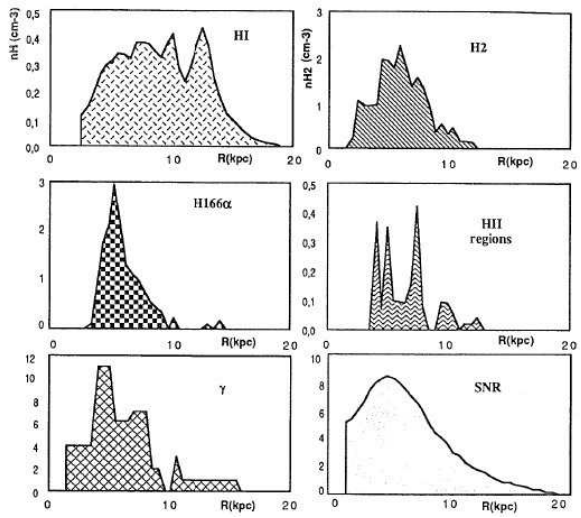

The distribution of different ISM components in Milky Way is typical for galaxies.

H166α: recombination line, traces H II regions
γ: brightness in γ-rays

Combes et al. (Fig. 2.6)

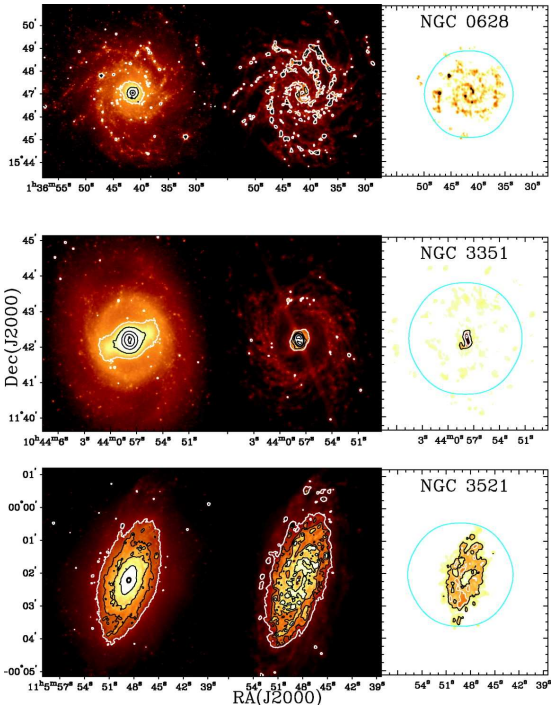

- Left: 3.6 μm: red giant stars
- Middle: 0.8 μm, star subtracted: PAHs
- Right: CO(1-0) mosaic (circle: outer range of detection)

(Regan et al., 2006, Fig. 1)

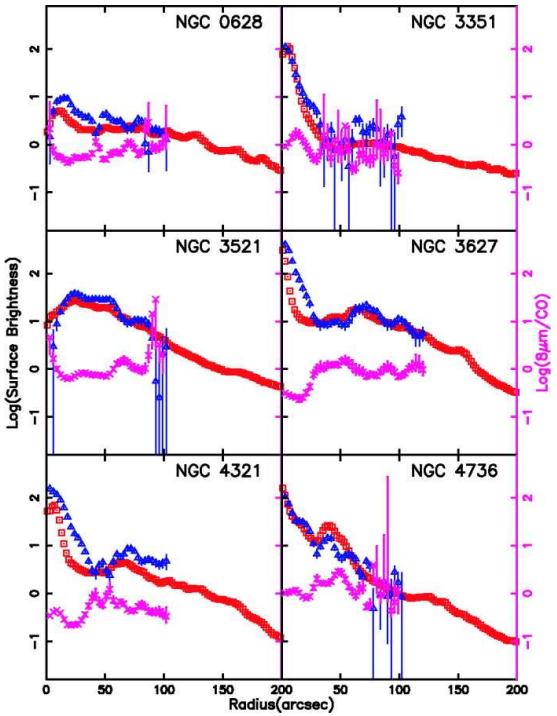

Radial intensity profiles:

- red: PAH
- blue: CO
- magenta: ratio

(Regan et al., 2006, Fig. 3)

Distribution of Gas and Dust

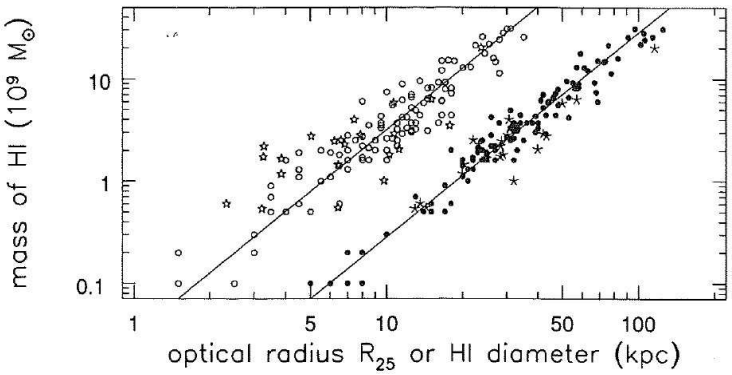

SG (Fig. 5.15)

- open circles: Mass of H I gas as function of R_{25} (note: $\propto R_{25}^2$; slope: 10 $M_\odot$ pc^{-2})
- filled circles: diameter where surface density drops to 1 $M_\odot$ pc^{-2} (slope: 3.6 $M_\odot$ pc^{-2} within diameter)

$\Longrightarrow$ H I disk extends generally to $\sim 2R_{25}$

Distribution of Gas and Dust

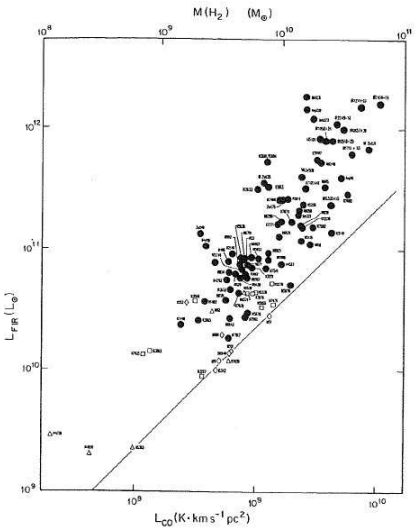

The IR luminosity and the CO luminosity (=H_2-content) of spirals are generally correlated.

Line: milky way

L_{IR}/M_{H_2}: good indicator for star formation, for normal spirals ratio is 1…3, for starbursts 20–30, for “IRAS-galaxies” can reach 200.

Combes et al. (Fig. 2.11)

Synchrotron radiation

Magnetic fields: trace through synchrotron radiation from electrons moving around B-field lines.

Lorentz-force (Gaussian units!):

$$\frac{d\boldsymbol{p}}{dt} = \frac{e}{c}\boldsymbol{v} \times \boldsymbol{B} \quad \text{where} \quad \boldsymbol{p} = \frac{m_\mathrm{e}\boldsymbol{v}}{\sqrt{1-\beta^2}} = \gamma m_\mathrm{e}\boldsymbol{v} \quad \text{with} \quad \gamma = \frac{1}{\sqrt{1-\beta^2}} \quad \text{and} \quad \beta = \frac{v}{c} \tag{4.4}$$

Therefore the acceleration is

$$\frac{d\boldsymbol{v}}{dt} = \frac{e}{c\gamma m_\mathrm{e}}\boldsymbol{v} \times \boldsymbol{B} \tag{4.5}$$

Since $\boldsymbol{v} \times \boldsymbol{B}$ is always perpendicular to $\boldsymbol{v}$ and $\boldsymbol{B}$, the component of $\boldsymbol{v}$ along the B-field does not change. This constant perpendicular force results to a helical motion around the B-field line with the frequency

$$\omega_B = \frac{eB}{\gamma m_\mathrm{e} c} = \frac{\omega_\mathrm{L}}{\gamma} \quad \text{with the Larmor frequency} \quad \omega_\mathrm{L} = 2\pi\nu_\mathrm{L} = \frac{eB}{m_\mathrm{e}c} \tag{4.6}$$

For typical ISM values, the Larmor frequency and Larmor radius are

$$\nu_\mathrm{L} = 2.8 \times 10^6 B_{10^{-6}\,\mathrm{G}}\,\mathrm{MHz} \quad \text{and} \quad R_\mathrm{L} = \frac{\gamma v_\perp}{\omega_\mathrm{L}} \sim 2\,\mathrm{AU} \cdot \frac{E}{1\,\mathrm{GeV}} \cdot \left(\frac{B}{10^{-6}\,\mathrm{G}}\right)^{-1} \tag{4.7}$$

Synchrotron radiation

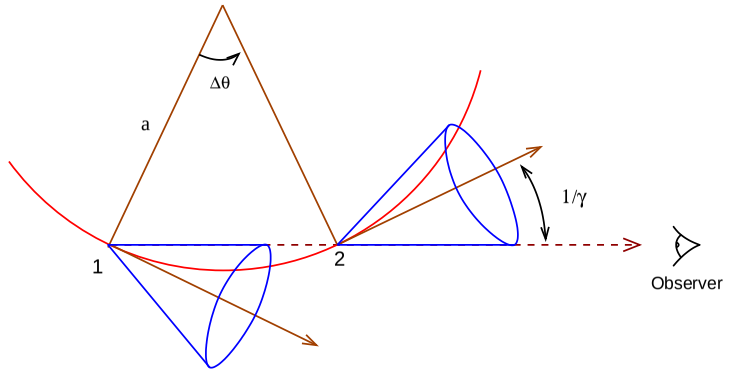

(after Fig. 6.2 of Rybicki & Lightman, 1979)

Electrons are accelerated, and therefore radiate. For relativistic electrons: radiation is forward beamed into cone with opening angle $\Delta\theta \sim 1/\gamma$. In the Electron frame of rest: beam passes observer during time

$$\Delta t = \frac{\Delta\theta}{\omega_B} = \frac{m_\mathrm{e}c\gamma}{eB}\frac{2}{\gamma} = \frac{2}{\omega_\mathrm{L}} \tag{4.8}$$

Synchrotron radiation

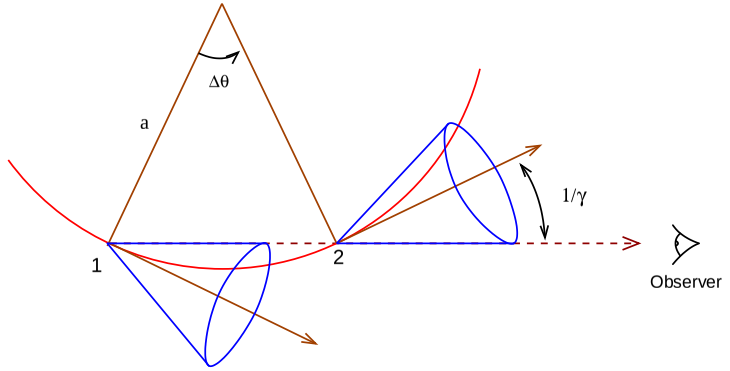

(after Fig. 6.2 of Rybicki & Lightman, 1979)

Observer frame: Doppler effect! (electron is closer to us at end of time interval)

$\Longrightarrow$ observed pulse duration:

$$\tau = \left(1 - \frac{v}{c}\right)\Delta t = (1-\beta)\Delta t \tag{4.9}$$

Synchrotron radiation

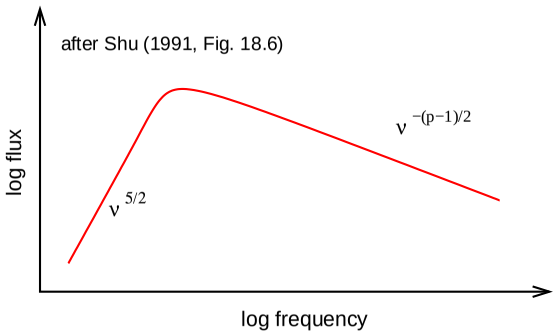

At low ν: synchrotron emitting electrons can absorb synchrotron photons:
synchrotron self-absorption.

For a power law electron distribution $\propto E^{-p}$, total spectral shape can be shown to be:

For low frequencies: $P_\nu \propto B^{-1/2}\nu^{5/2}$ (independent of p!)
For large frequencies: $P_\nu \propto \nu^{-(p-1)/2}$

One often uses the terms optically thick/thin to describe the absorbed/unabsorbed part of a synchrotron spectrum. The turnover describes the $\tau = 1$ surface, e.g., of a jet. In general: $\tau \propto R$ (R: size of the emitting region). More compact regions are optically thick, more extended regions are optically thin.

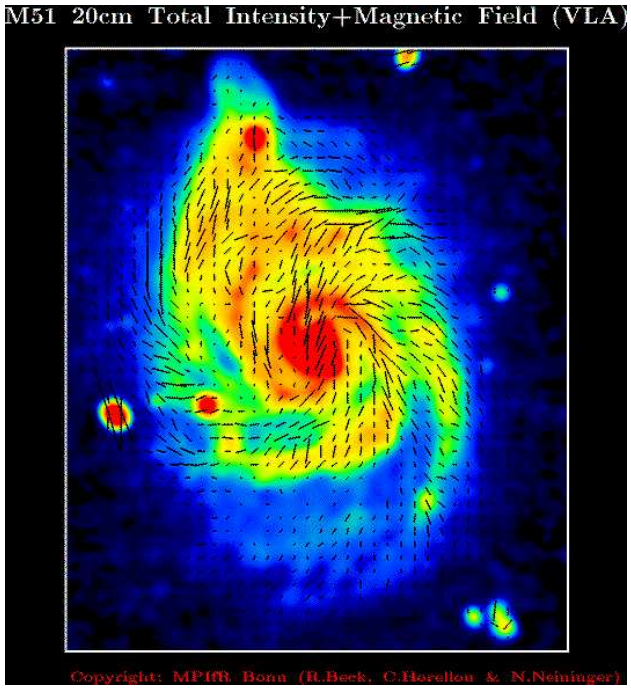

In addition to spectral shape, synchrotron radiation is strongly polarized.
Polarization can be used to find B-field vectors!

B-field vectors inferred from the degree of polarization in spiral galaxy M51 by rotation of the observed E-field-vectors by 90°

(Neininger 1992, A&A 263, 30)

Pagel B.E.J., 2009, Nucleosynthesis and Chemical Evolution of Galaxies, CUP, Cambridge, 2nd edition

Prantzos N., 2008, In: C. Charbonnel & J.-P. Zahn (ed.) Stellar Nucleosynthesis: 50 years after B2FH, Vol. 32. EAS Publ. Ser., p.311

Regan M.W., Thornley M.D., Bendo G.J., et al., 2004, ApJS 154, 204

Regan M.W., Thornley M.D., Vogel S.N., et al., 2006, ApJ 652, 1112

Rybicki G.B., Lightman A.P., 1979, Radiative Processes in Astrophysics, Wiley, New York

Seigar M., Carollo C.M., Stiavelli M., et al., 2002, AJ 123, 184

Shu F.H., 1991, The Physics of Astrophysics, Vol. I. Radiation, University Science Books, Mill Valley, CA